US006914441B2

(12) **United States Patent**
Talbot et al.

(10) **Patent No.: US 6,914,441 B2**
(45) **Date of Patent: Jul. 5, 2005**

(54) **DETECTION OF DEFECTS IN PATTERNED SUBSTRATES**

(75) Inventors: **Christopher G. Talbot**, Emerald Hills, CA (US); **Chiwoei Wayne Lo**, Campbell, CA (US)

(73) Assignee: **Applied Materials, Inc.**, Santa Clara, CA (US)

(*) Notice: Subject to any disclaimer, the term of this patent is extended or adjusted under 35 U.S.C. 154(b) by 0 days.

(21) Appl. No.: **10/134,210**

(22) Filed: **Apr. 29, 2002**

(65) **Prior Publication Data**

US 2002/0166964 A1 Nov. 14, 2002

Related U.S. Application Data

(60) Continuation of application No. 09/846,487, filed on Apr. 30, 2001, now Pat. No. 6,509,750, which is a division of application No. 09/226,967, filed on Jan. 8, 1999, now Pat. No. 6,252,412.

(51) **Int. Cl.**[7] **G01R 31/302**; G01N 23/00

(52) **U.S. Cl.** **324/750**; 250/310

(58) **Field of Search** 324/750, 751; 250/310, 311; 382/145

(56) **References Cited**

U.S. PATENT DOCUMENTS

3,638,015	A	1/1972	Browning et al.	250/49.5 A
3,701,979	A	10/1972	Smith et al.	340/173 R
4,068,218	A	1/1978	Likuski	365/237
4,342,949	A	8/1982	Harte et al.	315/409
4,415,851	A	11/1983	Langner et al.	324/51
4,417,203	A	11/1983	Pfeiffer et al.	324/51
4,443,278	A	4/1984	Zingher	156/64
4,567,402	A	1/1986	Mourier	315/39.3
4,575,630	A	3/1986	Lukianoff	250/307
4,712,057	A	12/1987	Pau	324/73

(Continued)

FOREIGN PATENT DOCUMENTS

EP	0309956	4/1989	G01R/31/28
EP	0853243	7/1998	G01R/31/305
JP	50795449	5/1984	H01L/21/66
JP	61362350	7/1985	H01L/21/66

OTHER PUBLICATIONS

Design and optimization of magnetic lenses and deflection systems for electron beams, E. Munro, *J. Vac. Sci Technol.*, 12(6), Nov./Dec. 1975, pp. 1146–1150.

(Continued)

Primary Examiner—David Zarneke
Assistant Examiner—Russell M Kobert
(74) *Attorney, Agent, or Firm*—Blakely, Sokoloff, Taylor & Zafman

(57) **ABSTRACT**

One embodiment of the present invention is a method of detecting defects in a patterned substrate, including: (a) positioning a charged-particle-beam optical column relative to a patterned substrate, the charged-particle-beam optical column having a field of view (FOV) with a substantially uniform resolution over the FOV; (b) operating the charged-particle-beam optical column to acquire images of a region of the patterned substrate lying within the FOV by scanning the charged-particle beam over the patterned substrate; and (c) comparing the acquired images to a reference to identify defects in the patterned substrate.

18 Claims, 11 Drawing Sheets

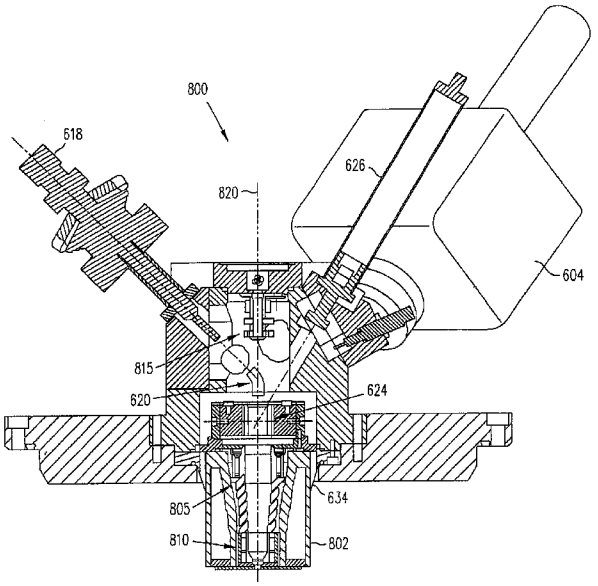

Patent provided by Sughrue Mion, PLLC - http://www.sughrue.com

U.S. PATENT DOCUMENTS

4,825,087	A		4/1989	Renau et al. 250/492.2
4,843,330	A		6/1989	Golladay et al. ..... 324/158 R
4,855,673	A		8/1989	Todokoro ..... 324/158 R
4,896,045	A		1/1990	Okunuki et al. 250/492.2
4,912,052	A		3/1990	Miyoshi et al. 437/8
4,939,360	A		7/1990	Sakai 250/251
4,943,769	A		7/1990	Golladay et al. ..... 324/158 R
4,972,083	A		11/1990	Taya et al. 250/281
5,030,908	A		7/1991	Miyoshi et al. ..... 324/158 R
5,057,773	A		10/1991	Golladay et al. ..... 324/158 R
5,089,710	A		2/1992	Kikuchi et al. 250/492.3
5,136,540	A		8/1992	Hayashi et al. 365/185
5,148,034	A		9/1992	Koike 250/492.2
5,187,371	A		2/1993	Matsui et al. ..... 250/396 R
5,214,289	A		5/1993	Betsui ..... 250/396 R
5,254,856	A		10/1993	Matsui et al. 250/310
5,304,801	A		4/1994	Arai 250/311
5,401,972	A		3/1995	Talbot 250/491.1
5,412,209	A		5/1995	Otaka et al. 250/310
5,420,433	A		5/1995	Oae et al. 250/398
5,442,183	A		8/1995	Matsui et al. 250/441.11
5,493,116	A		2/1996	Toro-Lira et al. 250/310
5,502,306	A		3/1996	Meisburger et al. 250/310
5,528,048	A		6/1996	Oae et al. 250/492.22
5,578,821	A		11/1996	Meisberger et al. 250/310
5,602,489	A		2/1997	El-Kareh et al. 324/75.1
5,614,725	A		3/1997	Oae et al. 250/492.22
5,777,327	A		7/1998	Mizuno 250/310
5,872,358	A		2/1999	Todokoro et al. 250/310
5,986,263	A		11/1999	Hiroi et al. 250/310
6,072,178	A		6/2000	Mizuno 250/310
6,172,363	B1	*	1/2001	Shinada et al. 250/310
6,187,687	B1		2/2001	Plat et al. 438/724
6,252,412	B1	*	6/2001	Talbot et al. 324/750
6,433,561	B1	*	8/2002	Satya et al. 324/753

OTHER PUBLICATIONS

MOL (moving objective lens) Formulation of deflective aberration free system, E. Goto et al., *Optik*, 48 1977, No. 3, pp. 255–270, month unavailable.

Recent Advances in Electron–Beam Lithography for the High–Volume Production of VLSI Devices, H.C. Pfeiffer, *IEEE Trans. Electr. Dev.*, vol. ED–26, No. 4, Apr. 1979, pp. 663–674.

Advanced deflection concept for large area, high resolution e–beam lithography, H.C. Pfeiffer et al., *J. Vac. Sci Technol.*, 19(4), Nov./Dec. 1981, pp. 1058–1063.

Variably shaped electron beam lithography system, EB55:II Electron optics, N. Saitou et al., *J. Vac. Sci Technol.*, 19(4), Nov./Dec. 1981, pp. 1087–1093.

Testing integrated circuit microstructures using charging–induced voltage contrast, T.J. Aton et al., *J. Vac. Sci Technol.*, B 8(6), Nov./Dec. 1990, pp. 2041–2044.

Analysis of Silicide Process Defects by Non–Contact Electron–Beam Charging, K.A. Jenkins et al., *30th annual proceedings reliability physics 1992*, 3/31, 4/1, 4/2, 1992, pp. 304–308.

The electrostatic moving objective lens and optimized deflection systems for microcolumns, M.G.R. Thomson, *J. Vac. Sci Technol.*, B 14(6), Nov./Dec. 1996, pp. 3802–3807.

Electron Beam Testing Technology Edited by J.T.L. Thong, *Plenum Press*, pp. 40–63, date unavailable.

Use of the Voltage Contrast Effect for the Automatic Detection of Electrical Defects on In–Process Wafers, T.R. Cass, KLA Yield Management Seminar, pp. 506–1 to 506–11, date unavailable.

* cited by examiner

Patent provided by Sughrue Mion, PLLC - http://www.sughrue.com

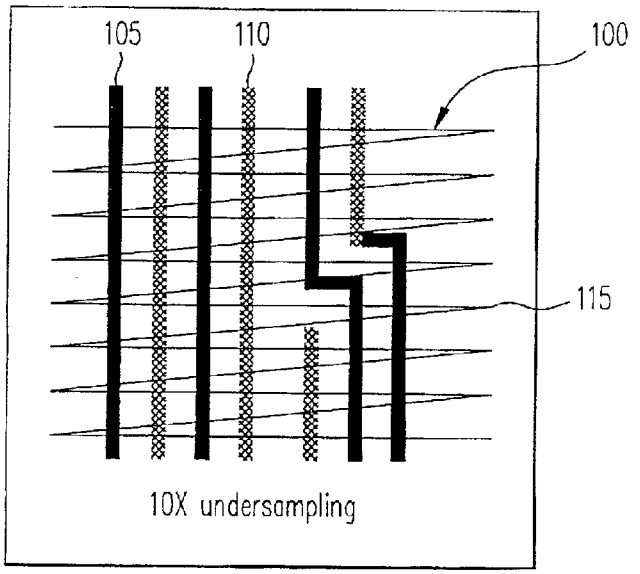

FIG. 1
(Prior Art)

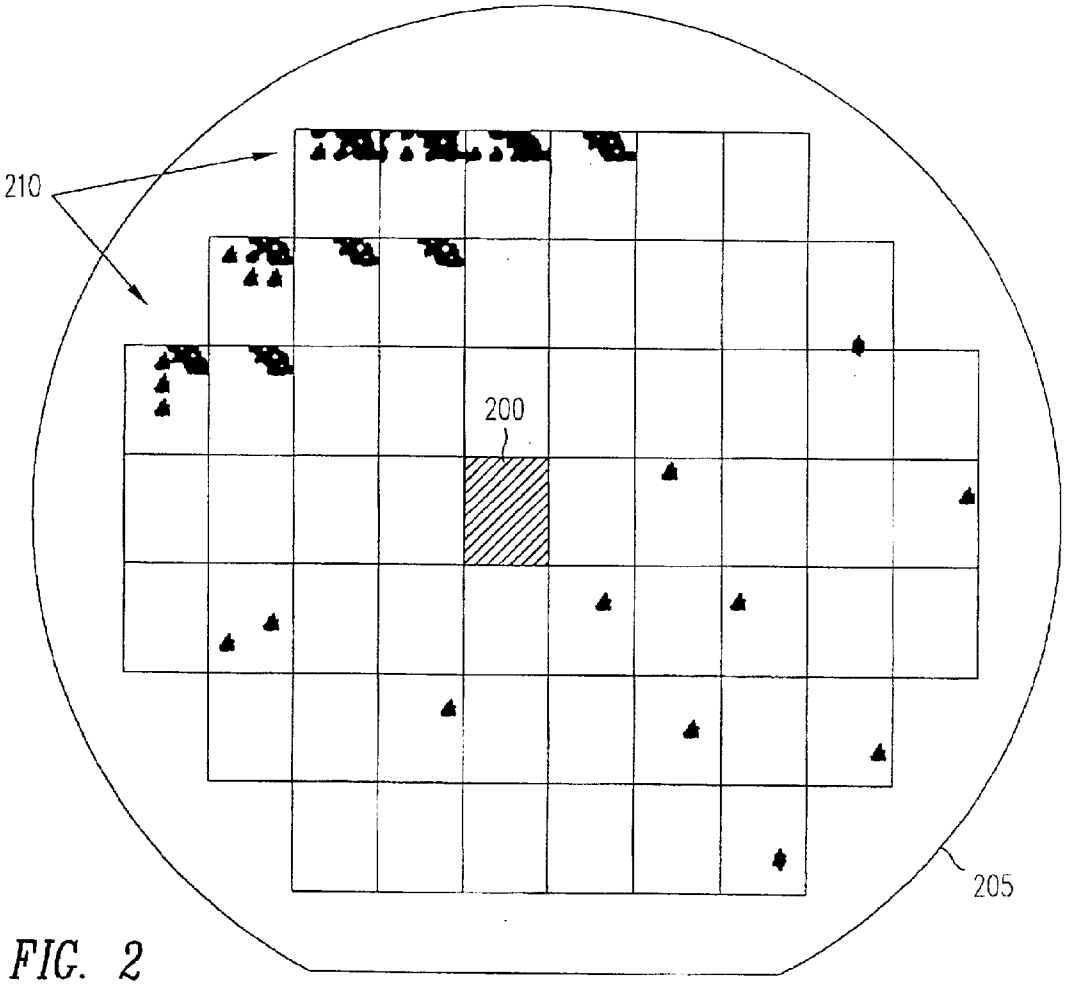

FIG. 2

Patent provided by Sughrue Mion, PLLC - http://www.sughrue.com

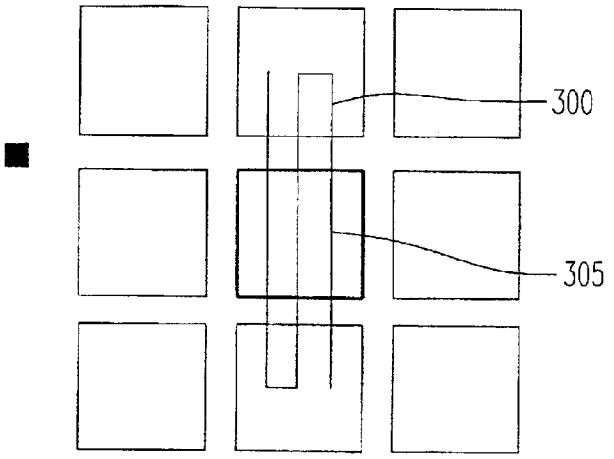

FIG. 3A
(Prior Art)

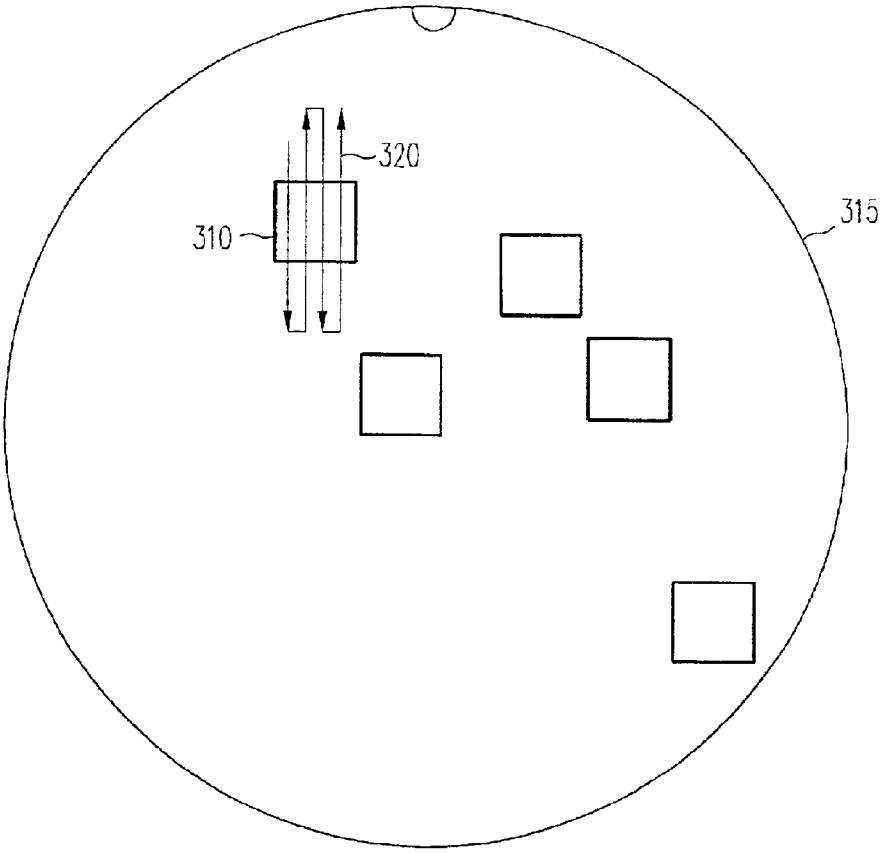

FIG. 3B
(Prior Art)

Patent provided by Sughrue Mion, PLLC - http://www.sughrue.com

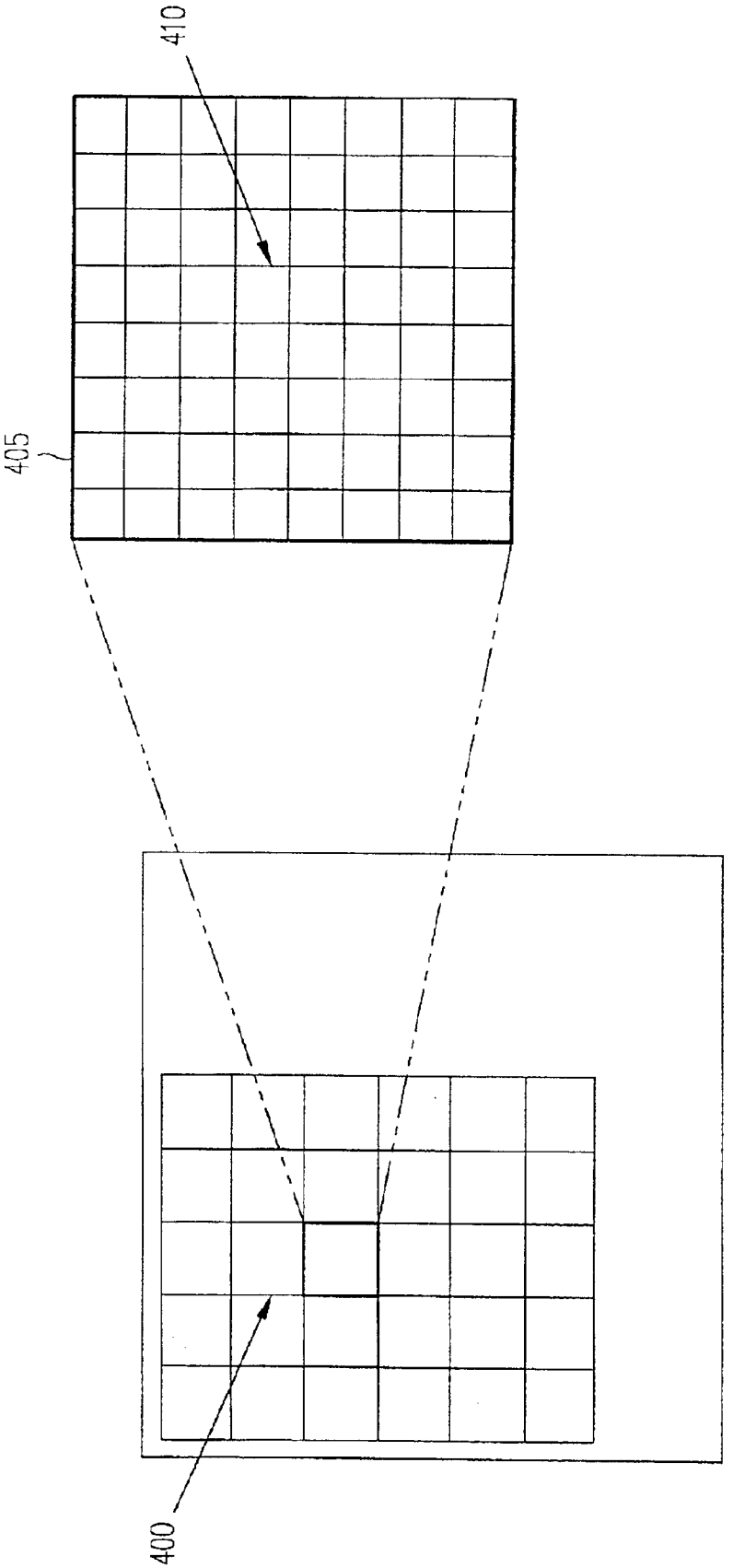

FIG. 4

Patent provided by Sughrue Mion, PLLC - http://www.sughrue.com

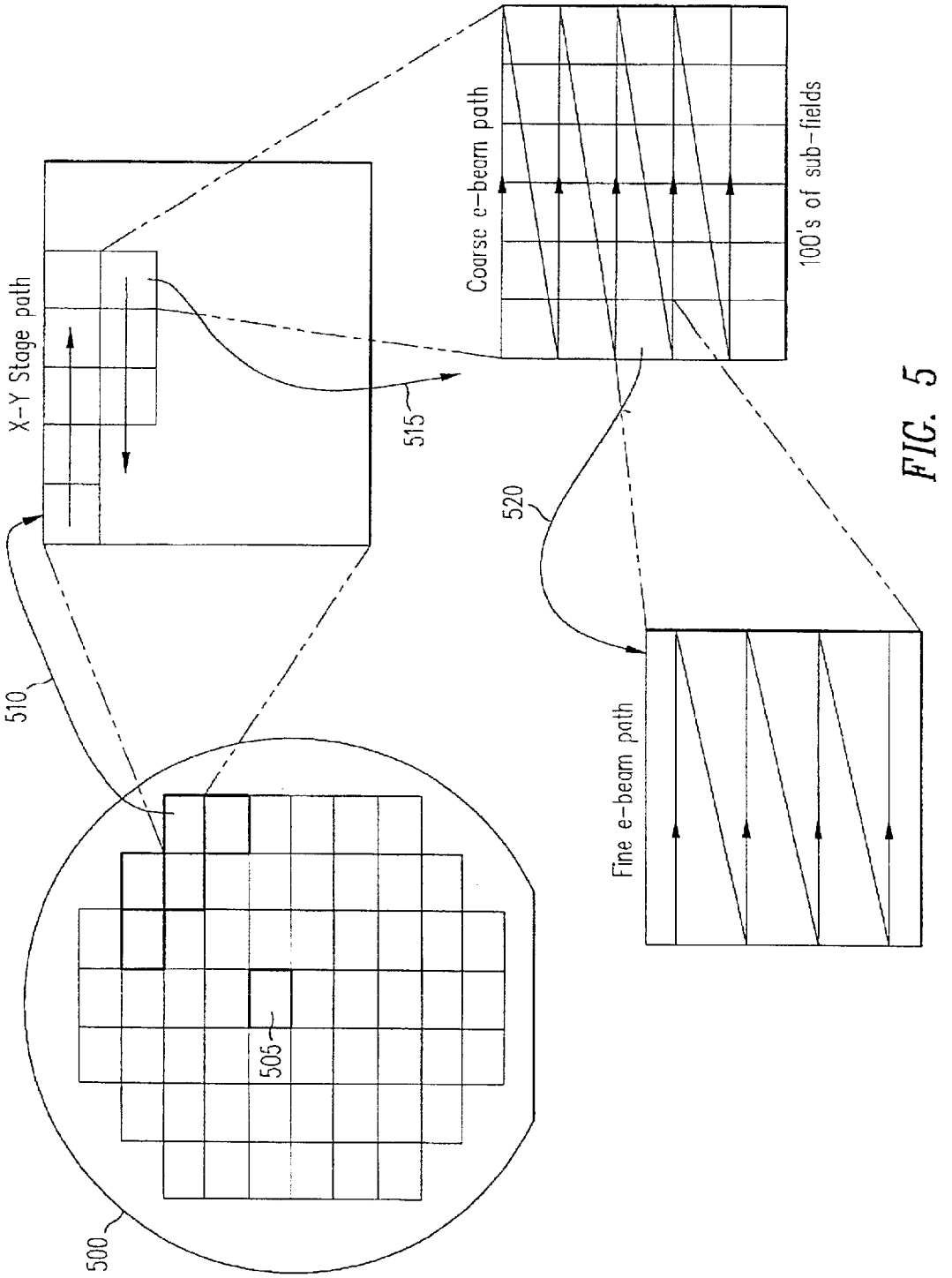

FIG. 5

Patent provided by Sughrue Mion, PLLC - http://www.sughrue.com

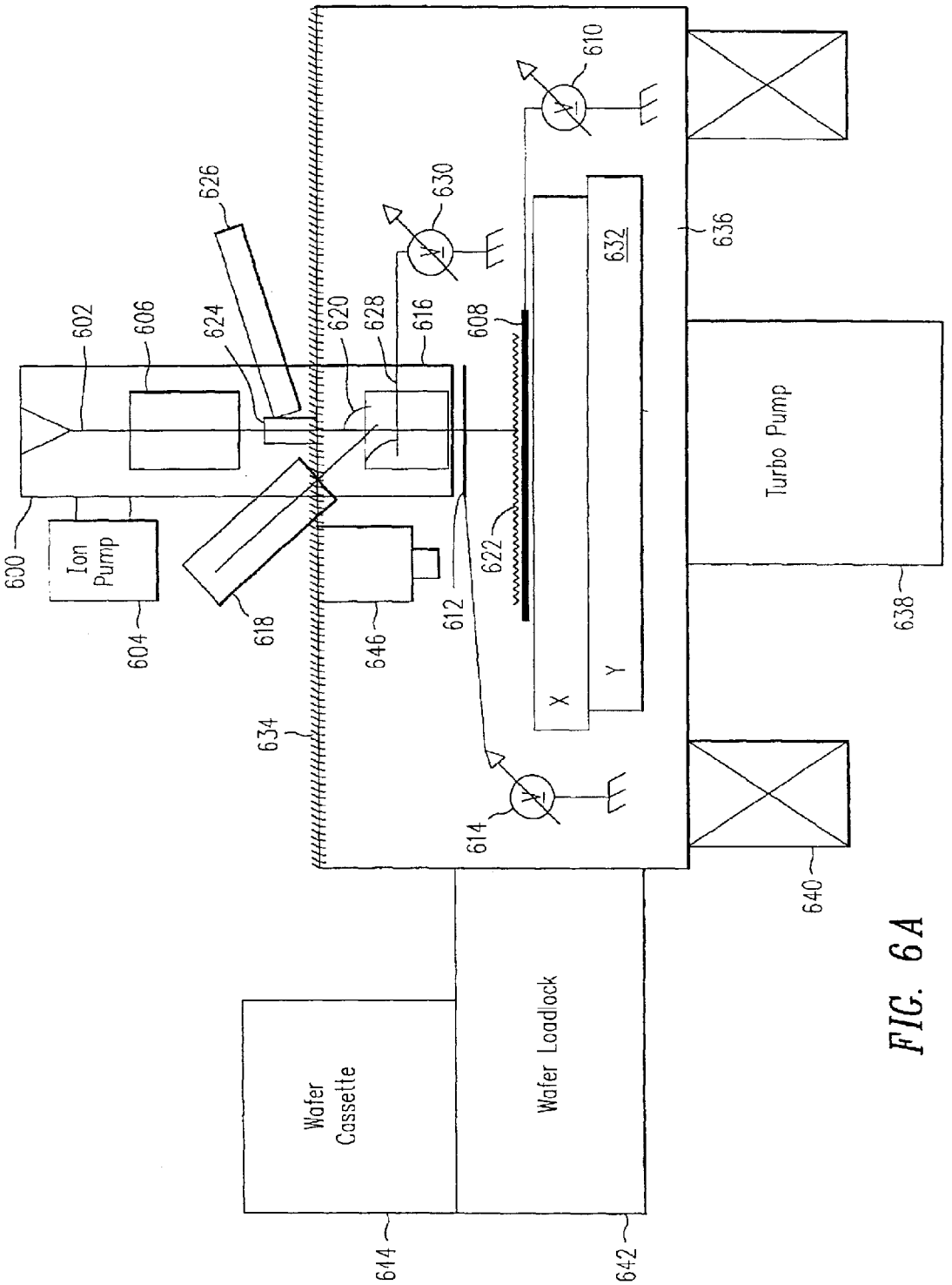

FIG. 6A

Patent provided by Sughrue Mion, PLLC - http://www.sughrue.com

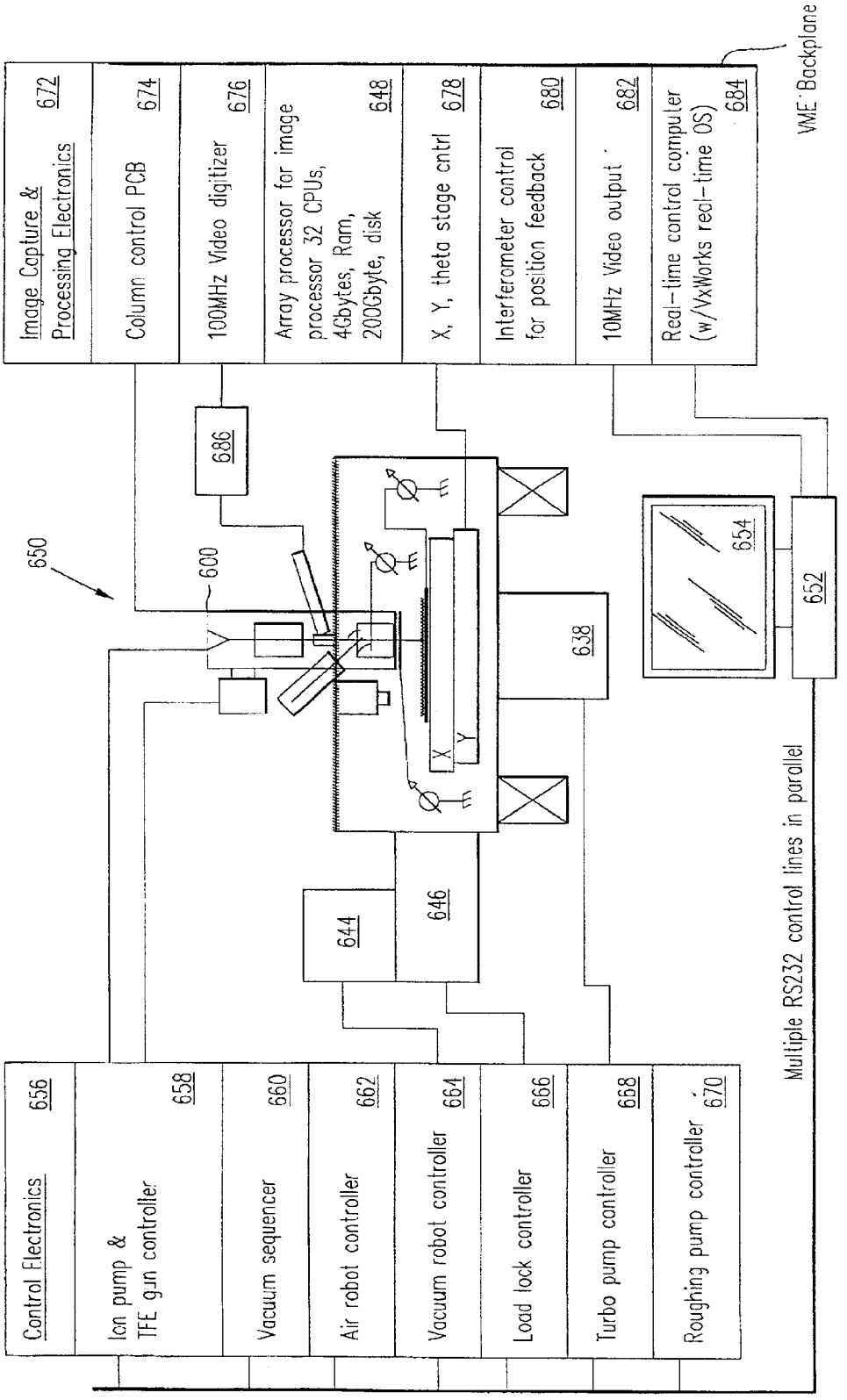

FIG. 6B

Patent provided by Sughrue Mion, PLLC - http://www.sughrue.com

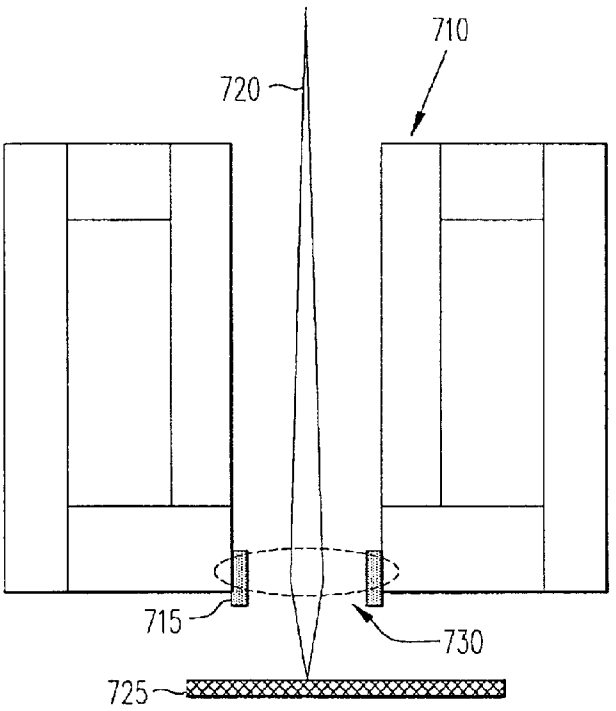

FIG. 7A

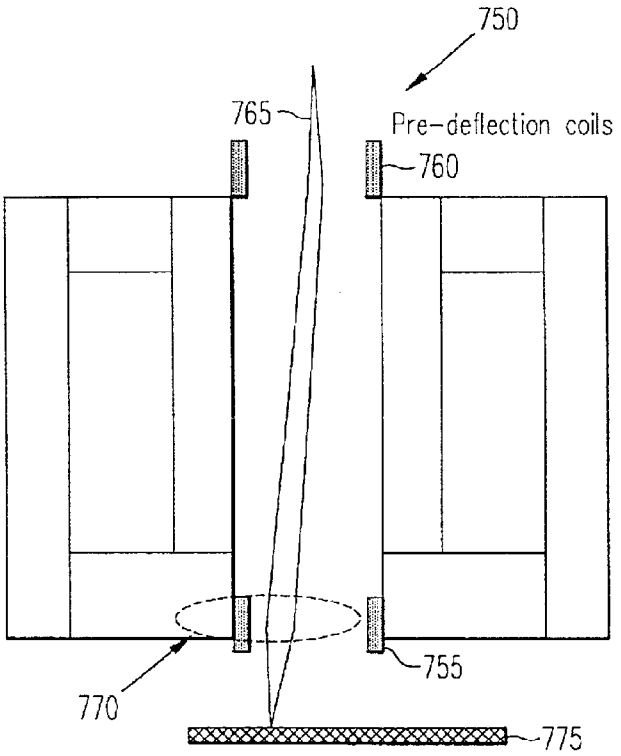

FIG. 7B

Patent provided by Sughrue Mion, PLLC - http://www.sughrue.com

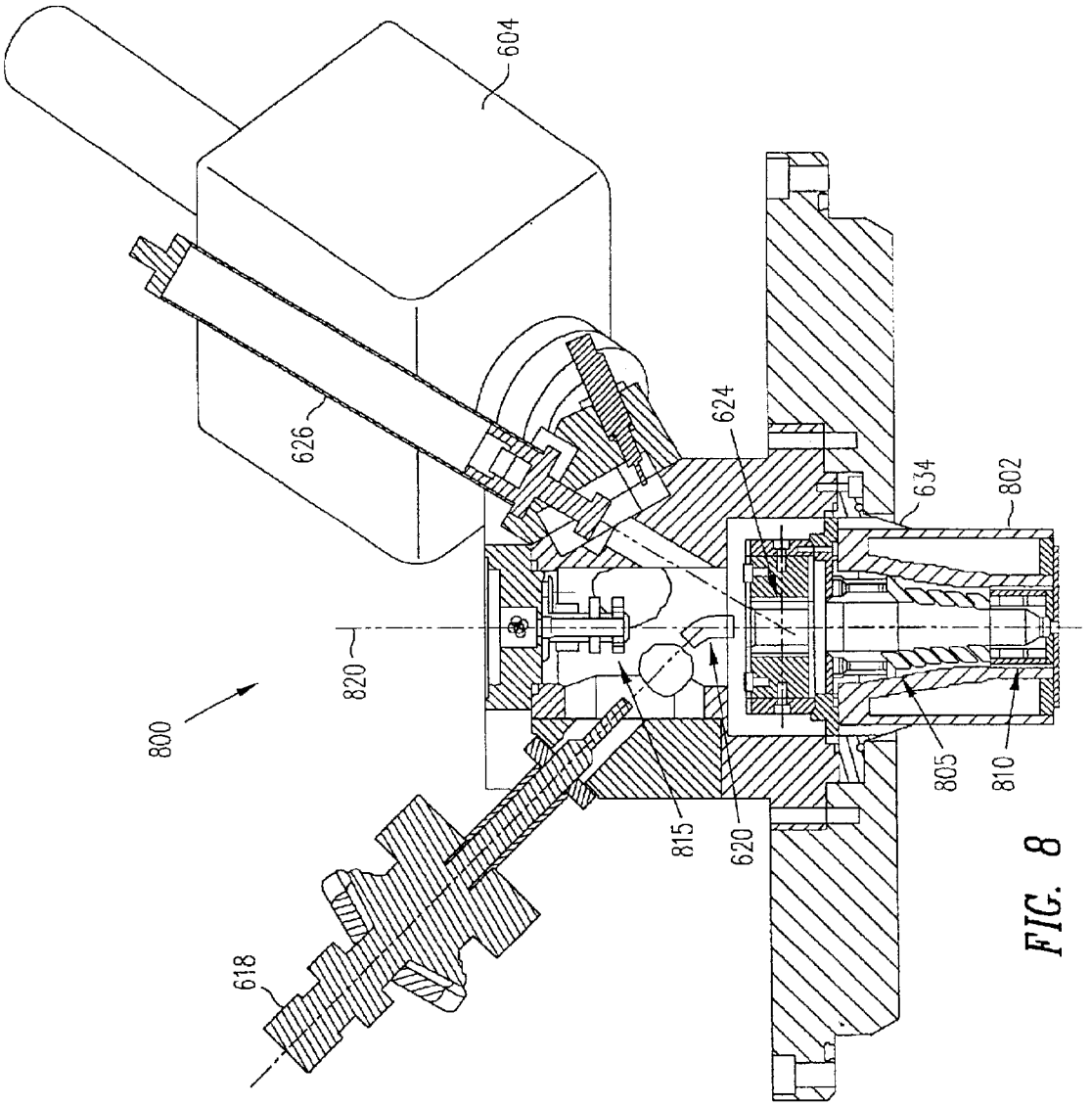

FIG. 8

Patent provided by Sughrue Mion, PLLC - http://www.sughrue.com

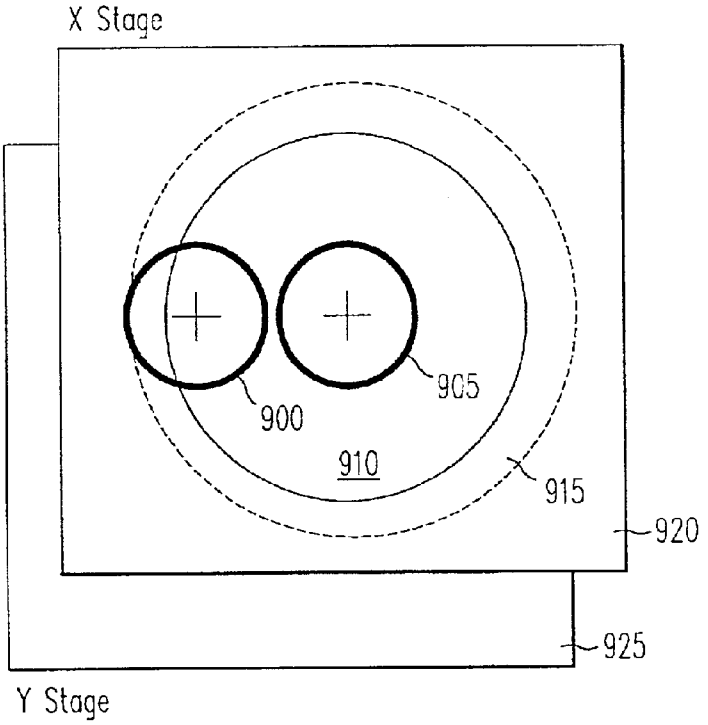

FIG. 9

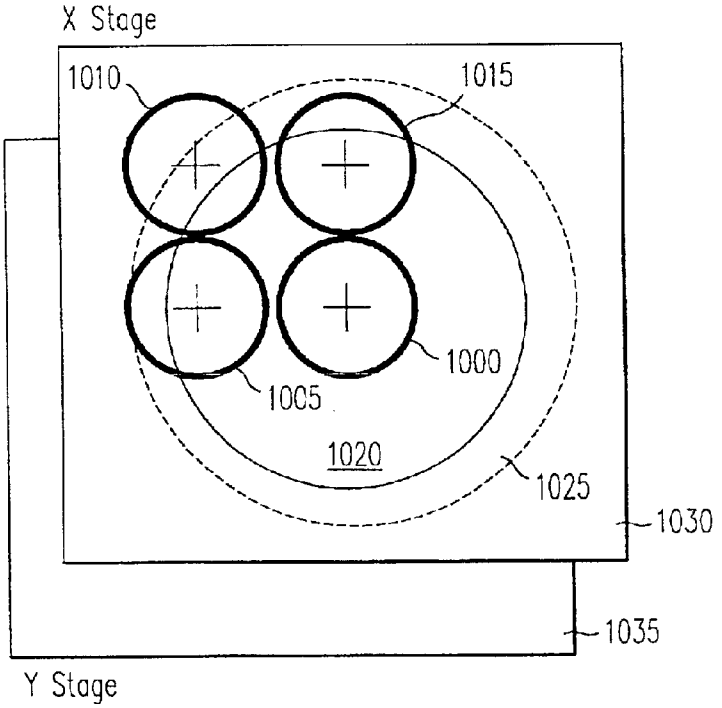

FIG. 10

Patent provided by Sughrue Mion, PLLC - http://www.sughrue.com

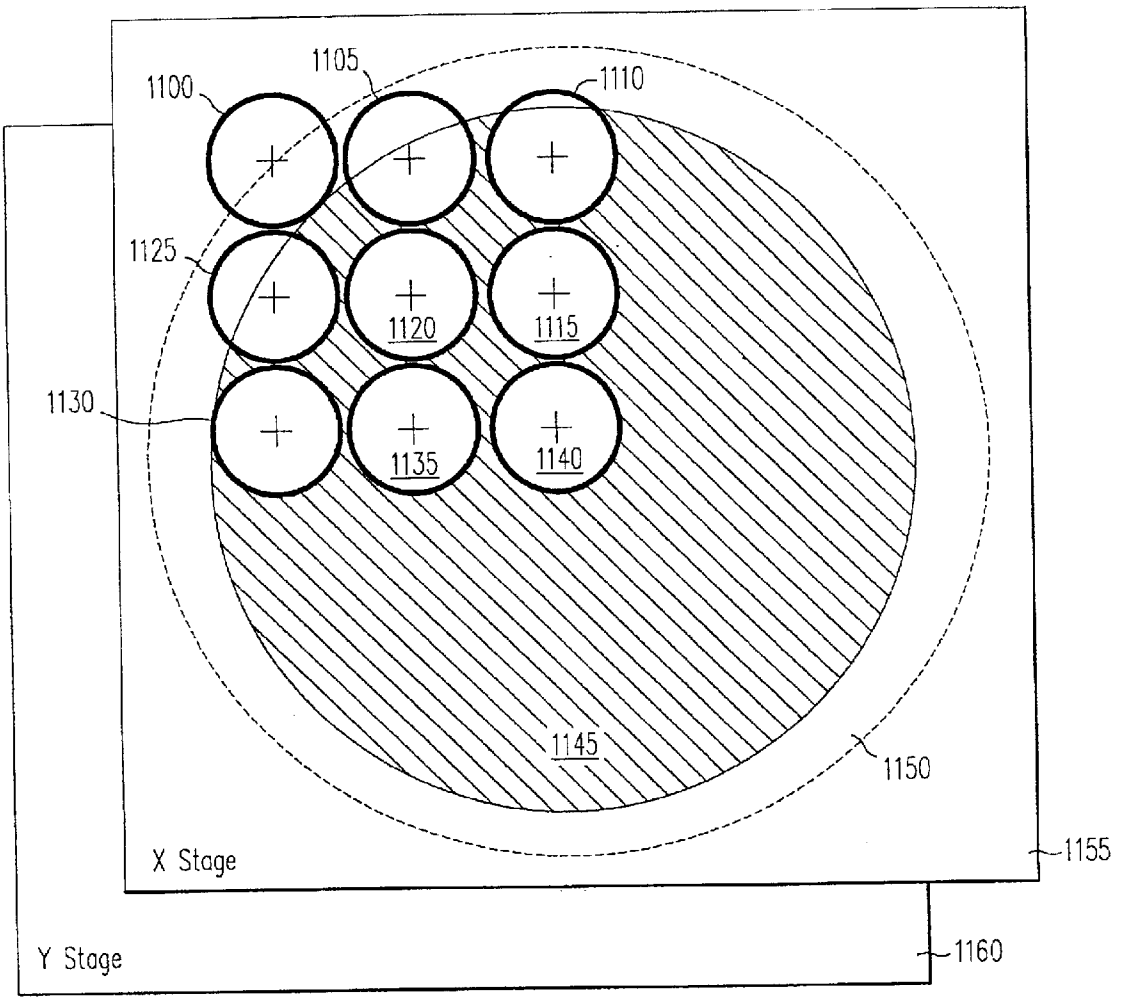

FIG. 11

Patent provided by Sughrue Mion, PLLC - http://www.sughrue.com

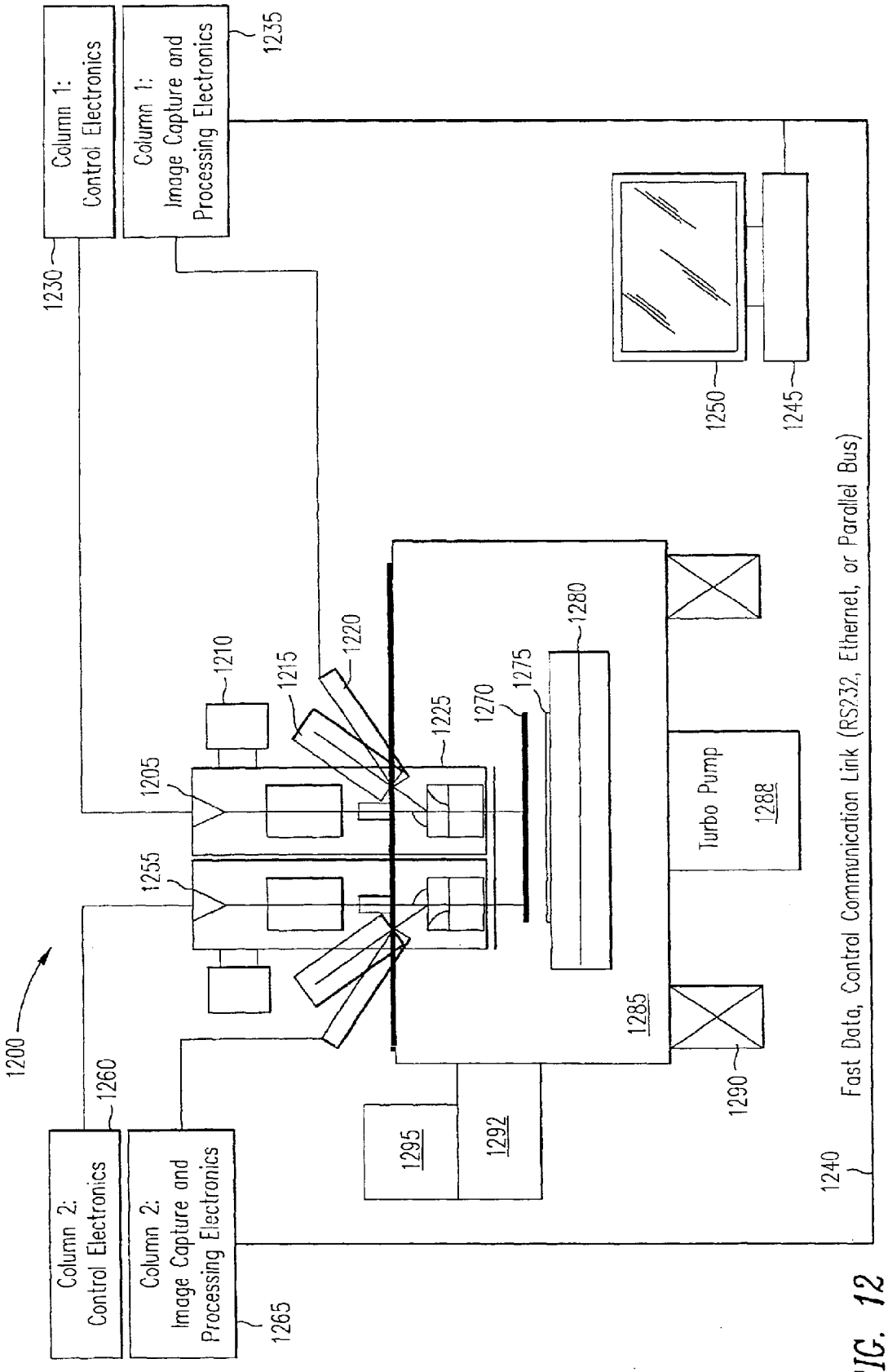

FIG. 12

Patent provided by Sughrue Mion, PLLC - http://www.sughrue.com

DETECTION OF DEFECTS IN PATTERNED SUBSTRATES

CROSS-REFERENCE TO RELATED APPLICATIONS

This application is a continuation of U.S. patent application Ser. No. 09/846,487, filed Apr. 30, 2001 now U.S. Pat. No. 6,509,750, which in turn is a divisional of U.S. patent application Ser. No. 09/226,967, filed Jan. 8, 1999, now U.S. Pat. No. 6,252,412, all incorporated by reference in their entireties.

This application is related to U.S. patent application Ser. No. 08/892,734 filed Jul. 15, 1997 now U.S. Pat. No. 6,504,393, U.S. patent application Ser. No. 08/782,740 filed Jan. 13, 1997 now abandoned, U.S. patent application Ser. No. 09/012,227 filed Jan. 23, 1998 now U.S. Pat. No. 6,162,621, U.S. patent application Ser. No. 09/226,962 filed on Jan. 8, 1999 now U.S. Pat. No. 6,232,787, and U.S. patent application Ser. No. 09/227,747 filed on Jan. 8, 1999 now U.S. Pat. No. 6,539,109, and U.S. patent application Ser. No. 09/227,395 filed on Jan. 8, 1999 now U.S. Pat. No. 6,344,750, all incorporated herein by reference in their entireties.

TECHNICAL FIELD OF THE INVENTION

One or more embodiments of the present invention relate to detection of defects in patterned substrates, such as semiconductor wafers, particularly by inspection using an electron beam.

BACKGROUND OF THE INVENTION

It is generally accepted that the most economical approach to increasing yields of semiconductor devices is to detect defects as early as possible during fabrication, rather than at final test of the devices. Early detection can allow a source of defects to be identified and eliminated before large numbers of wafers are affected. Thus, it is now standard industry practice to inspect wafers for defects at multiple stages of fabrication.

In-line inspection is now mostly done using optical inspection tools such as the 21XX-series wafer-inspection tools of KLA-Tencor. These employ a high-performance optical microscope, a fast scanning stage, a time-delay-integration, fast-scanning CCD image sensor, and a multi-processor image-processing computer. Algorithms are provided which perform pixel-by-pixel comparison of an optical image of a die against images of one or two neighboring die or dice, or pixel-by-pixel comparison of an optical image of a memory cell against neighboring memory cells. Other optical inspection systems are supplied, for example, by Applied Materials, formerly Orbot, and Hitachi.

Optical tools are inherently limited by diffraction and depth of focus. As a result, more than 50% of killer defects arising in processes using <0.35 μm design rules prove to be optically undetectable defects. Killer defects are defects which adversely affect electrical performance of a device at final test of the device. Trends indicate that this problem will become worse, especially for metal interconnect layers with sub-surface defects. This is due to the small depth of focus of conventional optical inspection tools, an inherent limitation of the large numerical aperture objective lenses required to image sub-micron features. Thus any defect that is not at the device surface will be substantially out of focus and therefore undetectable. Examples of such sub-surface defects include polysilicon gate shorts, open vias and contacts, and metal stringers. All of these result in either an electrical "open" or "short" type defect. Also, diffraction-limited resolution renders small surface defects undetectable as minimum critical dimensions (CDs) shrink below 0.25 μm. These include defects such as ~0.1 μm particles and regions of missing or extra pattern which are at or below the minimum CD.

Conventional scanning-electron-microscope (SEM) and electron-beam prober technology can image these small surface defects. E-beam probers can also "observe" (detect) subsurface defects by measuring the voltage-contrast change resulting from the electrical effect of killer defects, i.e., "open" and "short" type defects. See, for example: T. ATON et al., "Testing integrated circuit microstructures using charging-induced voltage contrast," J. VAC. Sci. TECHNOL. B 8 (6), November/December 1990, pp. 2041–2044; K. JENKINS et al., "Analysis of silicide process defects by non-contact electron-beam charging," 30th ANNUAL PROCEEDINGS RELIABILITY PHYSICS 1992, IEEE, March/April 1992, pp. 304–308; J. THONG, ED., ELECTRON BEAM TESTING TECHNOLOGY, Plenum Press 1993, p. 41; and T. CASS, "Use of the Voltage Contrast Effect for the Automatic Detection of Electrical Defects on In-Process Wafers," KLA Yield Management Seminar, pp. 506-2 through 506-11.

Conventional SEMs are too slow, however, to cover a statistically significant wafer area or number of defects in a short enough period of time. This limitation stems primarily from the slow serial nature of the data-collection process, though also in part from a general lack of automation. In addition the time taken to move the mechanical stage to each new imaging position is large compared to the imaging time and thus limits throughput even with automation features.

KLA's SEMSpec system is based on a conventional optical inspection system having a mechanical scanning stage. It uses a continuously-moving, accurate scanning stage together with a high-current beam and a high-bandwidth detector to increase the area-coverage rate. The scanning stage reduces stage-move time as a primary limiting factor in system throughput. The overall area-coverage rate of ~1 cm^2/hour with the SEMSpec system is substantially less that the several thousands of cm^2/hour with fully automated optical tools. See, for example, U.S. Pat. Nos. 5,502,306 and 5,578,821 to Meisburger et al.

U.S. patent applications Ser. No. 08/782,740 filed Jan. 13, 1997, and No. 09/012,227 filed Jan. 23, 1998 disclose another approach to obtaining higher rates of area coverage, at least for conductive layers. The conductive layers are pre-charged and then "under-sampled" where features are typically long, thin, co-parallel wires. For example, FIG. **1** illustrates pre-charged 10X undersampling of an IC layer **100** having conductors such as **105** and **110** oriented mostly in a single direction. The sample surface is precharged and only one of ten lines is sampled. Shown at **115** is the e-beam sampling scan path. The layout of a typical logic IC maximizes routing density by orienting conductors of alternate layers in mutually-orthogonal directions—conductors of one layer are routed mostly in the x-direction while conductors of adjacent layers are routed mostly in the y-direction. The pre-charged, under-sampling approach offers much benefit with layers having characteristics suited to under-sampling. It is unfortunately not as effective with layers having other characteristics, e.g., layers with small features such as vias, contacts, localized interconnects and memory cells. This approach is also unlikely to detect small particles or missing or extra patterns.

A result is that, in many situations, e-beam-based defect detection is only feasible with full imaging rather than

Patent provided by Sughrue Mion, PLLC - http://www.sughrue.com

undersampling. Full-imaging with an area-coverage rate of 1 cm^2/hour would take an estimated ~270 hours to cover all of a typical 200 mm-diameter wafer. To improve throughput, it is instead desirable to selectively sample areas of the wafer that are expected to have the most defects of interest. It is also advantageous to be able to compare against any reference die, or against a database, rather than against only a neighboring die as is the case with scanning-based optical inspection systems currently in use and with the SEMSpec system.

The ability to compare an image of a die against any reference allows sampling of the wafer area to be targeted at a specific defect distribution. For example, comparing the center die of a wafer, which is more likely to be defect free, with edge dice, which are often expected to have higher defect densities, maximizes the likelihood of detecting such defects. Figure illustrates a desired sampling scenario tailored for a specific defect distribution, but which is not addressed by prior art systems. In this example a center die **200** of wafer **205** is selected as a reference and is compared to outlying die **210** which are more likely to have defects. Comparing a die to an adjacent die would be less likely to show all the defects.

It is believed that commercially available e-beam defect detection systems only look at memory arrays by comparing one memory cell against its neighbors. While a scanning stage-based system might be used to perform a die to any die comparison, the scanning stage turn-around time would be a primary overhead factor limiting throughput. FIGS. **3**A an **3**B illustrate the effect of state turn-around time.

FIG. **3**A shows the path **300** of a continuously moving stage (not shown) relative to an area **305** of a wafer being scanned. Image data is acquired while the stage is moving at a constant velocity. The average rate of data acquisition is reduced by the time required for the mechanical stage to decelerate, reverse direction, and accelerate to scanning speed, and the time required to realign the beam with the sample. FIG. **3**B illustrates the overscan resulting from use of a continuously moving scanning stage. To scan an area **310** of wafer **315** at a constant velocity, the stage must move beyond the edge of the scanned area **310** for deceleration, reversal, and acceleration. The scan path of the stage relative to area **310** is shown at **320**.

A goal for a charged-particle-beam defect-detection system to be used in a production environment is to minimize or eliminate stage overhead so that acquisition speed is limited by the fundamental physics of the beam, thus taking best advantage of charged-particle beam technology to detect optically undetectable defects (OUDs).

In general, a wide range of potential reference image sources can be used, each having relative advantages and disadvantages in specific applications. The most versatile approach it to have complete flexibility in sampling and choice of reference without compromising throughput. Presently available systems lack such flexibility. Following is a description of some desired comparisons.

Comparison	Comments
Cell to Cell	Typically used for memory cells. A perfect reference cell may be used to compare to every cell in a memory array, or each memory cell (or repeating structure such as a block of or 4 symmetrically-reflected cells) is compared with its neighbor.

-continued

Comparison	Comments
Die to die	This is typically a standard mode of operation for an optical inspection system such as the KLA213X. Each die is compared to its adjacent neighbor during the scanning process. A third die is then used to arbitrate which die actually has the defect. This works well for random defects but not for repeating defects such as extra pattern in a tightly-routed section of the mask. In general, it is preferred to have the capability to efficiently compare any die with any die, using any third die for arbitration. Die to any die comparisons are valuable because the user can target specific areas of the wafer with a particular expected defect type and compare against a die that is likely to be good. Edge die to center die comparison on a semiconductor wafer is desirable for this reason, since edge die are often "weak" and less likely to yield than center die.
Die to golden die	An image or other data from a known-good reference die ("golden" die) on another wafer is stored in memory and compared to the die under inspection. A large volume of data is required, literally hundreds of gigabytes, but disk and memory space is becoming less costly and there is potential for image compression of voltage contrast images. No arbitration is required when comparing with a "golden" die.
Die to database	This technique is known for inspection of masks, such as in KLA's mask inspection systems. A challenge with the apparent-feature enlargement approach is that multiple layers of the database and knowledge of the electrical properties of the circuit represented are required to determine which features are grounded and which are floating in negative charge mode, e.g., which p-n junctions are forward biased by the negative potential or voltage.
Block to block	Similar to die to die but just some subsection(s) of the die are compared. This is useful when a portion of the die is known or expected to be more likely to have a particular type of defect of interest. This approach saves time over full die-to-die comparison.

Conventional SEM columns are optimized for best imaging performance for a relatively small Field of View (FOV), typically within 1 μm to 100 μm of the column's optical axis. Mechanical stages move the sample wafer and column relative to one another to allow viewing of the complete sample. This is acceptable in applications where throughput is not a major concern, and is believed to be the norm in commercial SEMs. Particle-beam systems are known to operate over a large field of view (FOV) for purposes such as e-beam lithography, but not for defect detection. See, for example, H. PFEIFFER, "Recent Advances in Electron-Barn Lithography for the High-Volume Production of VLSI Devices," IEEE TRANSACTIONS ON ELECTRON DEVICES, Vol. ED-26, No. 4, April 1979; and N. SAITOU et al., "Variably shaped electron beam lithography system, EB55: II ELECTRON OPTICS," J. VAC. SCI. TECHNOL., 19(4), November/December 1981. It is also known to use a large FOV for overlay alignment, as in U.S. Pat. No. 5,401,972 to Talbot et al. and in Schlumberger's commercially-available IDS P2X and AMS systems.

Improved systems and methods are needed for detection of defects on a patterned substrate.

SUMMARY OF THE INVENTION

One or more embodiments of the present invention solve one or more of the above-identified issues in the prior art. In particular, one embodiment of the present invention is a method of detecting defects in a patterned substrate, comprising: (a) positioning a charged-particle-beam optical column relative to a patterned substrate, the charged-particle-

Patent provided by Sughrue Mion, PLLC - http://www.sughrue.com

beam optical column having a field of view (FOV) with a substantially uniform resolution over the FOV; (b) operating the charged-particle-beam optical column to acquire images of a region of the patterned substrate lying within the FOV by scanning the charged-particle beam over the patterned substrate; and (c) comparing the acquired images to a reference to identify defects in the patterned substrate.

BRIEF DESCRIPTION OF THE FIGURE

FIG. **1** illustrates pre-charged 10X undersampling of an IC layer having conductors oriented mostly in a single direction;

FIG. **2** illustrates a typical sampling scenario tailored for a specific defect distribution;

FIG. **3**A illustrates stage movement with a continuously moving stage;

FIG. **3**B illustrates overscan resulting from use of a continuously moving stage;

FIG. **4** illustrates an image-acquisition scheme consistent with the invention;

FIG. **5** further illustrates an image-acquisition scheme consistent with the invention;

FIG. **6**A schematically illustrates the column, stage and chamber section of a defect-detection system consistent with the invention;

FIG. **6**B schematically illustrates the high-level architecture of a defect-detection system consistent with the invention;

FIG. **7**A illustrates the effective lens position of a lens having single deflection coils;

FIG. **7**B illustrates the effective lens position of a moving-objective lens having dual deflection coils;

FIG. **8** is a cross-sectional view of a large-FOV objective lens useful in a defect-detection system consistent with the invention;

FIG. **9** shows a schematic, plan view of a defect-detection system consistent with the invention having two columns ganged together for simultaneously imaging multiple regions of a wafer;

FIG. **10** shows a schematic, plan view of a defect-detection system consistent with the invention having four columns ganged together for simultaneously imaging multiple regions of a wafer;

FIG. **11** shows a schematic, plan view of a defect-detection system consistent with the invention having nine columns ganged together for simultaneously imaging multiple regions of a wafer; and

FIG. **12** shows a schematic view of a defect-detection system **1200** consistent with the invention having two columns ganged together for simultaneously imaging multiple regions of a wafer.

DETAILED DESCRIPTION

A goal for e-beam-based defect detection is to minimize the effect of stage-move-time and settling-time overhead in the overall time needed for the system to acquire image data. System throughput in the most versatile imaging-mode of operation should be limited only by the physics of interaction between the e-beam and the sample. It is also desirable to compare any die or die portion on the wafer to any other die or die portion on the wafer or to a stored reference image from another wafer or a CAD database, without significantly degrading system throughput.

One or more embodiments of the present invention address this need by using a large-FOV objective lens having substantially constant resolution over the large FOV. Mechanical-stage overhead is minimized by using the e-beam as a near-ideal mini-stage, similar to a mass-less stage in the field of light optics. For each mechanical stage position, images are acquired at multiple sub-fields of view (sub-FOVs). Because e-beam deflection, alignment and settling times are negligible compared to the image acquisition time for a single sub-FOV, the time required to move from one image-acquisition area to another is substantially eliminated. Because a large number (~100s) of sub-FOVs can be acquired for each mechanical stage position, the time required for mechanical stage movement and settling is negligible compared to the total acquisition time for a complete lens FOV encompassing hundreds of sub-FOVs. Hence the effect of stage-movement overhead is a small part of the total time needed to acquire images at many regions of a wafer.

One embodiment of the present invention is a high-speed defect-detection system that is suitable for inspection of semiconductor wafers before fabrication is completed. It employs a large field of view (FOV) objective lens to reduce the time overhead associated with mechanical-stage moves. The main FOV of the lens, covering for example a region of mm ×~1 mm, is sub-divided into hundreds of sub-FOVs. The system can acquire images of a sample within each sub-FOV without the need for a mechanical-stage move. An in-lens detector is optimized for collecting and detecting secondary electrons efficiently and uniformly across the full FOV of the large-FOV objective lens. We term this a "step-and-image" technique, as distinguished from prior-art techniques employing substantially-continuous stage motion during image acquisition.

FIG. **4** and FIG. **5** illustrate principles of an image-acquisition scheme in accordance with the present invention. Shown in FIG. **4** is an example of applying the large-FOV objective lens in a step-and-image technique to acquire tiled images from a single die. Region **400** of a wafer contains a die or die portion to be inspected. Region **400** can be divided as shown at **405** into multiple sub-regions, such as 1 mm by 1 mm sub-regions. Each of these sub-regions represents a FOV of a large-FOV e-beam column; for a given position of the mechanical stage which establishes relative position between the sample wafer and the e-beam column, the e-beam column is capable of acquiring images over a corresponding large-FOV sub-region. With the mechanical stage positioned for image acquisition over sub-region **410**, the e-beam can be scanned to acquire images over many sub-FOV areas, typically hundreds of sub-FOV areas. With the mechanical stage held stationary, the e-beam can be stepped nearly instantaneously between sub-FOV areas for image-acquisition scanning within sub-FOV areas.

FIG. **5** illustrates an example of using a large-FOV e-beam column to acquire images for detecting defects on a wafer **500**. In this example, an image of a center die **505** is acquired and used as a reference image for comparison with images of several edge dice, such as edge die **510**. The mechanical stage is moved to a position such that a die portion **515** can be imaged by the large-FOV e-beam column without further movement of the mechanical stage. Die portion **515** contains many, e.g., hundreds, of sub-FOVs. The e-beam is directed to the vicinity of a sub-FOV such as sub-FOV **520**, and is scanned over the sub-FOV so as to acquire an image of the sub-FOV region of the die.

One or more embodiments of the present invention have the potential for relatively simple implementation. Prior-art large-FOV lithography systems use complex dynamic-focus and aberration-correction schemes to overcome changes in

Patent provided by Sughrue Mion, PLLC - http://www.sughrue.com

lens aberrations as the beam is moved across the full FOV. Such complex schemes are not required for defect detection in accordance with one or more embodiments of the present invention because only a finite number of specific sub-FOV images are used for acquisition of a particular image. A lookup-table approach can thus be used to statically correct the focus and the aberrations at each FOV. Interpolation between entries in the lookup table can also be used to reduce the size of the lookup table.

One or more embodiments of "step and image" techniques in accordance with the present invention can provide throughput and implementation advantages for voltage-contrast-based defect detection as well as the conventional surface-or topographic-imaging-based defect detection using an e-beam. The following examples illustrate overhead and throughput advantages of a system employing a large-FOV lens and a stepping stage relative to a prior-art system using a small-FOV lens and a continuously-scanning stage for inspecting a single die on a wafer.

EXAMPLE 1

The following typical parameters are assumed for "Case 1" and "Case 2":

- die size=1 cm^2
- pixel resolution=25 nm
- pixel rate=100 MHz
- FOV of small-FOV lens 25 μm×25 μm (1,000 pixels per line, same as the sub-FOV of large-FOV lens)
- FOV of large-FOV lens=1 mm×1 mm
- time for a single stage move=1 second
- time for scanning stage to reverse direction and re-accelerate to constant speed=~3 seconds

Case 1: Time to acquire image of a single die using large FOV lens with step and image mode (consistent with the present invention)

Stage-Move Overhead:	100 stage moves =	100 seconds
Data acquisition time:	acquire 16×10^{10} pixels =	1600 seconds
Total time required:	stage moves + acquisition =	1700 seconds
Efficiency (data acquisition time/ total time):		1600/1700 = 94%

Case 2: Time to acquire image of a single die using small FOV lens with a continuously scanning staging (prior art)

Stage-Move Overhead:	time to reverse stage direction & re-accelerate 800 times =	2400 seconds
Data acquisition time:	acquire 16×10^{10} pixels =	1600 seconds
Total time required:	stage moves + acquisition =	4000 seconds
Efficiency (data acquisition time/ total time):		1600/4000 = 40%

EXAMPLE 2

As indicated in Table 1 below, this example assumes a 1 mm×1 mm FOV for the large-FOV objective lens and a 40 MHz pixel-data acquisition rate. The time for the stage to move and settle is conservatively assumed to be 1 second (typically a well-designed stepping stage would move and settle in <0.5 second). With these assumptions, the stage move overhead represents ~3% of the total image acquisition time. That is, an ideal stage which would move and settle instantaneously would only result in only a ~3% through-put increase. Thus the stage-move overhead is of little consequence.

TABLE 1

Critical Dimension(CD) =	0.18 μm	No pre-charge	
Pixels/CD =	4	Data rate =	4.00E + 07Hz
Pixel size =	0.045 μm	Avg. =	2
Pixels/cm =	222222	Time/sub FOV =	0.05 s
Pixels/cm =	49382716049	Beam vector time =	200 μs
		Total time/sub FOV =	0.05 s
FOV(per side) =	1 mm	Tinx/FOV =	24.8 s
FOV/cm^2 =	100		
Pixels/FOV line =	22222	Stage move/settle time =	1 s
Pixels/sub FOV line =	1000	Overhead (focus, etc) =	0.15
Sub FOV/line =	22.2	Total time/FOV =	25.9 s
Sub FOV size =	45 μm	Total time/cm^2 =	2589.012346/65
Sub FOV/FOV =	493.8	Total time/cm^2 =	0.71917009 6 hrs
		Data vol./Lg FOV =	1036 MB

A system consistent with the present invention for e-beam-based detection of defects in patterned wafers is shown schematically in FIG. **6**A and FIG. **6**B. FIG. **6**A shows the column, stage and vacuum-chamber section of the system. FIG. **6**B shows high-level system architecture. Referring to FIG. **6**A, electron-optical column **600** has an electron source **602** such as a Thermal Field Emission (TFE) electron source of the type used in most modern SEMs, for example with a zirconium-tungsten cathode. The electron source includes an electron gun (not shown) pumped directly by an ion pump **604**. High vacuum in the electron gun is separated from the rest of the column and chamber by a differential pumping aperture (not shown), as in most modern scanning-electron microscopes (SEMs). The primary beam landing energy is adjustable, for example in the range from 700 eV to 1.5 keV. Beam current at the specimen is adjustable, such as with a condenser lens **606** and beam limiting aperture (not shown), for example in the range from ~500 pA to ~10 nA, or even up to 25–50 nA into a spot size of <0.1 μm. Electron-optical column **600**, together with wafer-chuck **608** having a bias source **610** and extraction electrode **612** having a bias source **614**, form a Local Charge Control Module (LCCM).

Electron-optical column **600** includes a large Field Of View (FOV) objective lens **616**, such as a Variable Axis Immersion Lens (VAIL). Objective lens **616** can be a VAIL lens similar to that used in the Schlumberger ATE IDS 5000 and IDS 10000 e-beam probing systems. For example, the lens is a magnetic-immersion type where the specimen is held approximately at the point of maximum axial magnetic field. The field of such a lens acts as a "magnetic bottle" and allows for collimation and efficient collection of secondary electrons without the need to apply a strong electrostatic collection field. A strong electrostatic collection field is undesirable as it may cause unstable surface charging, and can preclude independent optimization of the wafer bias, extraction potential and energy filter to enhance voltage contrast. The lens can be equipped with both pre-deflection and deflection coils to achieve a large FOV (such as 0.25 mm to 1.5 mm across) with high resolution (such as 30–100

Patent provided by Sughrue Mion, PLLC - http://www.sughrue.com

nm). In one embodiment, a FOV of 0.25–1.5 mm across has been demonstrated with resolution of <50 nm. An embodiment of a VAIL lens in accordance with the present invention is described below with reference to FIG. **8**.

As shown schematically in FIG. **6**A, the objective lens assembly is equipped with an "In-The-Lens" flood gun **618** and a flood-beam bending electrode **620** that allows fast multiplexing between a broad, high-current flood beam for pre-charging the specimen and its conductors, and a high-resolution primary-imaging beam for fast imaging to interrogate the charge states of the specimen's conductors. Fast imaging is performed, for example, at a pixel acquisition rate of 10 MHz to 100 MHz. Flood gun implementation is described in U.S. patent application Ser. No. 08/782,740 filed Jan. 13, 1997, and Ser. No. 09/012,227 filed Jan. 23, 1998. Flood gun **618** in combination with the wafer chuck **608** having bias **610** and extraction electrode **612** having bias **614** form a Global Charge Control Module (GCCM).

Secondary electrons and, in general, other secondary particles are generated at the surface of the specimen **622** by raster-scanning the primary beam over the surface. These secondary electrons and other secondary particles are collected by the lens field, travel back through the bore of the lens and are separated from the primary electron beam by a Wien filter **624**. A Wien filter has crossed magnetic and electric fields. Secondary electrons are then detected by an electron detector **626**, such as a scintillator-PMT combination, also known as an Evahart-Thomley detector. Other detector combinations can also be used. Provision is advantageously made to shield the electron detector against damage or rapid aging from the strong secondary electron current generated when the flood beam is in use. The detector supplies a signal which can be used to form an image of the scanned region of the specimen.

In the embodiment of FIG. **6**A, provision is made to apply independent bias voltages to extraction electrode **612** from bias source **614** and to wafer chuck **608** from bias source **610**. Bias voltage applied to wafer chuck **608** is effectively applied also to the substrate of wafer **622**. These bias voltages can be independently set, under computer control if desired, to optimize voltage contrast depending on the type of wafer being imaged and the type of defect to be detected. As described in more detail in U.S. patent application Ser. No. 08/892,734 filed Jul. 15, 1997, the system can be operated to produce either a positive or a negative specimen-surface voltage. The wafer bias can also be used to independently vary the beam-landing energy at the specimen's surface; this is desirable as some specimens with thin layers such as salicide require low landing energy without compromising resolution, to prevent charge leakage to other layers from beam punch-through.

In the embodiment of FIG. **6**A, the bore of the lens is equipped with a planar filter electrode **628**, also called an energy-filter mesh, having a bias voltage source **630**. Electrode **628** serves as a retarding-field electron-energy spectrometer, as in the Schlumberger IDS 5000 & IDS 10000 systems. The energy filter can be used to optimize voltage contrast for certain wafer types by collecting secondary electrons with a specified energy range, for example in the range from zero to ~15 eV.

The embodiment of FIG. **6**A also includes an x-y stage **632**, which can be a high-speed stage equipped to handle wafers up to 300 mm diameter, allowing inspection of the entire upper surface of the wafer. The wafer is supported on a chuck **608** such as an electrostatic-type chuck. In general, the stage used should be suitable for use in a vacuum environment, non-magnetic to minimize unwanted beam deflection, clean-room compatible and reasonably accurate. There is a direct trade-off between stage accuracy and image alignment software overhead. For a "step-and-image" mode of operation in accordance with one or more embodiments of the present invention, a key performance goal is fast, accurate stepping with a short settling time after each mechanical step/move. The stage should thus be capable of high-speed operation as well as precise scanning and stepping operation, to enable detection of the widest possible range of defects. For example, the stage may have a settling time of <0.3 second, a linear speed of 100 mm/second, and laser-interferometer feedback for positional accuracy within ~0.1 μm. To assure such high stage-position accuracy, the mechanical path between stage **632** and electron-optical column **600** must be sufficiently rigid. In one embodiment, the roof **634** of vacuum chamber **636** is used as a metrology plate, fabricated of 5 inch thick aluminum re-enforced with an external H-frame. Electron-optical column **600** and precision stage **632** can be directly mounted on the metrology plate to minimize relative motion. A laser interferometer (not shown) can be used to provide accurate position feedback to the stage's motor controllers (not shown). More subtle position errors, also detected by the interferometer, are readily corrected by small deflections of the e-beam.

In the embodiment of FIG. **6**A, vacuum chamber **636** is pumped directly by a turbo pump **638** and an oil-free backing pump (not shown). As illustrated, vacuum chamber **636** is mounted on an active vibration isolation platform **640** which cancels environmental vibration and also predictively cancels motion due to fast acceleration and deceleration of mechanical stage **632**. A wafer load-lock subsystem **642** is included to minimize wafer change over time and to allow the main vacuum chamber to stay at high vacuum, such as IE-6 Torr, for long periods. Maintaining vacuum also minimizes hydrocarbon contamination of the wafer.

Wafer load-lock subsystem **642** includes wafer-handling robots for automatic loading and unloading of wafers. For example, a first robot moves wafers from a wafer cassette **644** to a load-lock chamber. After the load-lock is evacuated, robot operating in the vacuum environment of the vacuum chamber places the wafer on chuck **608** of precision stage **632**. The load-lock chamber advantageously is designed to accommodate several wafers to facilitate pipeline operation and simultaneous loading and unloading of wafers. Wafer-load-lock subsystem **642** can also advantageously include an optical wafer pre-aligner to provide a degree of wafer alignment accuracy relative to stage **632**.

Additional optical elements can be provided to more accurately align the wafer on the precision stage, such as an optical pre-alignment subsystem **646** having an optical microscope and CCD video camera for providing optical images to a pattern matching system. The pattern matching system can take the form of suitable software, from Cognex or another vendor, running on a processor to determine the actual position of the wafer relative to the precision stage. Alignment using e-beam images is sometimes possible, though for some semiconductor process layers, fiducial marks on the wafer and die can appear in low contrast in the e-beam image. This can make e-beam image-based alignment unreliable. Optical microscopes can see through insulating layers such as SiO_2, Si_3N_4 and make alignment more robust.

Referring to FIG. **6**B, data processing for image alignment and image comparison is carried out in an image-processing subsystem **648**, such as a multiprocessor-array computer from Mercury Computer Systems of Chelmsford,

Patent provided by Sughrue Mion, PLLC - http://www.sughrue.com

Mass. Image-processing subsystem **648** includes video input and output boards, an array of processors, random-access memory, and a large disk store. For example, image-processing subsystem **648** may comprise an array of thirty-two 300 MHz Power PC processors, 4 Gbytes of RAM and a ~200 Gbyte disk store for storage of reference images and defect data. Image-processing subsystem **648** can be programmed to execute a range of image processing algorithms including but not limited to: cell-to-cell comparison for memories, die-to-die comparison or die-to-reference for random logic, and feature-based comparison for contacts and other layers. Feature-based comparison is described in more detail, for example, in U.S. patent application Ser. No. 09/227,747 filed on Jan. 8, 1999.

A defect-detection system **650** as illustrated in FIG. **6**B includes a control computer **652**, such as a personal computer having a display **654** and a Pentium processor running the Windows NT operating system and system control software (not shown). Defect detection system **650** also includes control electronics **656** under control of computer **652** for providing signals to operate the described system elements. Defect-detection system **650** advantageously includes a multi-level, easy to use, graphical user interface (not shown) to support use by operators in an automated-factory environment based on pre-defined stored defect detection recipes as well as by engineers, typically having a higher skill set, in a laboratory or process-development environment. Software can be provided for functions such as system control, image processing, automatic beam setup, beam alignment, auto-focus and auto-astigmatism correction.

Control electronics **656** includes, for example, an ion-pump and TFE-gun controller **658**, a vacuum-sequencer **660**, an air-robot controller **662**, a vacuum-robot controller **664**, a load-lock controller **666**, a turbo-pump controller **668**, and a roughing-pump (backup-pump) controller **670**.

In the implementation of FIG. **6**B, image-processing subsystem **648** forms part of image-capture processing electronics **672**, which also includes an electron-optical-column controller **674**, a video digitizer **676**, a mechanical-stage controller **678**, an interferometer controller **680** for mechanical-stage-position feedback, a video output stage **682** for supplying an image signal to control computer **652** for display, and a real-time control computer **684** having a real-time operating system such as VxWorks or the like. The signal from electron detector **626** (FIG. **6**A) is supplied to a low-noise video amplifier **686**, which may have autofocus signal capability and which passes the electron-detector signal to video digitizer **676**.

As discussed in E. MUNRO, "Design and optimization of magnetic lenses and deflection systems for electron beams," J. VAC. Sci. TECHNOL., Vol. 12, No. 6, November/December 1975, pp. 1146–1150, the design allows beam deflection for raster scanning while achieving a large FOV. Possible design approaches can be classified into the following types: (1) post lens single deflection, (2) pre-lens double deflector, (3) single in-lens deflection, (4) single in-lens deflection, and (5) double in-lens deflection. A primary concern is that the beam travel through the lens center so that off-axis aberrations are minimized. This requirement sets restrictions on the size of the achievable field of view if resolution is not to be severely limited. To overcome this restriction, techniques like variable axis lens (VAL), described in H. PFEHFM et al., "Advanced deflection concept for large area, high resolution e-beam lithography," J. VAC. Sci. TECH., 19(4), November/December 1981, pp. 1058–1063, movable objective lens (MOL), described in E. GOTO et al., "MOL (moving objective lens): Formulation of deflective aberration free system," OPTIK 48 (1977) No. 3, pp. 255–270, and other variations described in M. THOMSON, "The electrostatic moving objective lens and optimized deflection systems for microcolumns," J. VAC. Sci. TECH. B 14 (6), November/December 1996, pp. 3802–3807, employ at least one set of pre-deflectors to steer the beam off-center, then implement a way to compensate the effects of the beam traveling off-center, for example, dynamically move the effective position of the lens.

When the beam is far-off the center axis of the lens, it experiences a strong repulsive force caused by the lens field. That force tends to bend the beam back toward the lens center. This is the basic reason why the lens can focus. This bending force not only makes the raster area extremely small but also introduces severe aberrations; for instance, transverse chromatic aberrations, coma, astigmatism, etc., for off-axis operation. Compensation or correction of these aberrations is key to designing a large field of view lens and is accomplished by placing a second set of deflectors near the lens. These deflectors generate a field to offset or balance the lens bending field. The lens behaves as if its optical center were moved even though mechanically (physically) it remains fixed.

Off-axis aberration correction in this manner allows practical implementation of a large field of view lens without suffering a loss of resolution from severe off-axis aberration.

FIG. **7**A and FIG. **7**B illustrate the principle of a Movable Object Lens (MOL). Lens **710** shown schematically in FIG. **7**A has a single set of deflection coils **715**, capable of focusing beam **720** at the surface of a sample **725**. The "effective" lens position is indicated by the dashed oval line **730**. Aberrations result when the beam is deflected off-axis by deflection coils **715**. Lens **750** shown schematically in FIG. **7**B has a set of deflection coils **755** as well as a set of pre-deflection coils **760**. Because beam **765** is pre-deflected by coils **760**, the "effective" lens position can be shifted as indicated by the dashed oval line **770**. The lens of FIG. **7**B behaves as if its optical center were displaced, reducing off-axis aberration and producing substantially constant resolution over a large FOV of sample **775**.

One possible implementation of an electron-optical column **800** including a large-FOV objective lens consistent with the invention is shown in cross-sectional view in FIG. **8**. The large-FOV objective lens is similar to that used in Schlumberger's IDS 5000 e-beam probing system. While only a single set of deflection coils was used or required for the IDS 5000 system, the lens design of FIG. **8** includes a two sets of coils, sometimes referred to as saddle coils: pre-deflection coils **805** to steer the beam off the optical axis of the objective lens, and deflection coils **810** generating a field to optimize the lens transverse field, corresponding to the lens bending force described above, so that off-axis aberrations are reduced. Because the direction and magnitude of this transverse field is proportional to the beam location relative to the lens center, the field generated by the 2^{nd} deflector has to be adjusted accordingly to approximately balance that of the 1^{st} deflector while minimizing total aberration(s), as is standard in the design of any lens. In operation, the 1^{st} and 2^{nd} deflectors are raster scanned in tandem to generate images. The balance between the two vector fields can be accomplished by using a fixed winding ratio and fixed rotation angle between the 1^{st} and 2^{nd} deflector coils. Alternatively, the balance can be achieved by electronically setting the excitation ratio and rotation angle between the two deflectors. A commercially-available, charged-particle optics simulation package from MEBS

Patent provided by Sughrue Mion, PLLC - http://www.sughrue.com

Software, Cornwall Gardens, London, UK, has been successfully used to simulate and optimize such a lens design. The embodiment of FIG. **8** further includes alignment and astigmatism correction coils **815**. The primary beam is shown at **820**. Electron-optical column **800** produces a beam spot size of, for example, <0.1 μm across a 1 mm field of view.

In the embodiment shown in FIG. **8**, no attempt is made to correct for the non-vertical beam landing angle, in contrast to e-beam lithography machines. A primary goal is to maximize the usable FOV so as to minimize the effect of stage-move time on system overhead when acquiring images from various regions of a sample. Accepting a non-vertical landing angle simplifies the design as no collimator lens is used (i.e., not telecentric) and only one pre-deflector is employed (i.e., the beam is not parallel to the lens axis). The beam landing angle can be up to ~15 degrees from the normal, which is acceptable for wafer inspection applications today. Any slight contrast variation can also be corrected by image normalization by using standard image processing routines.

High collection efficiency is key to this application as ultimately throughput is limited by shot noise and signal image averaging time. Reduced collection efficiency would result in proportionately slower throughput.

More details can be found in U.S. patent application Ser. No. 09/227,395 filed on Jan. 8, 1999, the contents of which have been incorporated herein by reference.

Image Processing and Image Alignment:

Once the images are acquired, image alignment and comparison is performed to detect defects. Each image is typically aligned to correct for misalignment for residual stage errors. Once aligned images, can be differenced in a number of ways:

- conventional pixel-to-pixel subtraction in which each pixel of an image is subtracted from the corresponding pixel in a reference image. The resulting difference image then shows any real defects (image differences) as well as nuisance information caused by subtle but real differences between the images that are not killer defects. Image processing techniques such as feature erosion (dilation and expansion) can be used to minimize or eliminate those of the nuisance defects which are smaller than a selected size;
- feature-based comparison in which the images are segmented into individual blobs or features for comparison on a feature-by-feature basis, such as described in co-pending U.S. patent application Ser. No. 09/227,747, filed on Jan. 8, 1999. Feature-based comparison is most valuable when the expected nuisance defects and actual defects are comparable in size, such as with contacts and vias. It also has the advantage of allowing spatial averaging to reduce shot noise beyond that achieved by temporal image averaging. An advantage is that more suitable voltage-contrast differences can be reliably differentiated without increasing the rate of nuisance defects.

Defect-detection methods and apparatus consistent with the invention can provide some implementation advantages:

- Minimize stage overhead while maintaining flexibility to sample small portions of a wafer without compromising system throughput.
- Avoid the need for an expensive scanning stage, allowing implementation with a relatively low-cost, low-accuracy stage because image-processing alignment can be used to avoid the need for accurate stage encoders.
- Use of sub-FOVs to avoid the need for dynamic focus and astigmatism correction on-the-fly using the full FOV of a large-FOV lens. With the sub-FOV approach described, a simple lookup table of lens operating parameters can be set for each sub-FOV.
- Pre-defined sub-FOVs can be used with a static lookup table to avoid dynamic alignment correction, with interpolation as appropriate between points in the pre-characterized look-up table. This approach can be used to compensate for mechanical alignment errors between the two deflection elements.
- Avoid dynamic rotation correction in a similar manner.
- Elegant, relatively simple and lower cost to implement than a traditional e-beam wafer inspection system such as the SEMSpec system.

Those of skill in the art will recognize that a variety of operating sequences consistent with the invention are possible. Following are a few examples:

1. Step-and-image, with no pre-charge flood and no multiple images per stage position

Load wafer, pump down, align wafer, align die
Set up imaging parameters, focus, astigmatism, area to be imaged
REPEAT:
acquire & store image
IF reference image available (can be done while stage is moving)
align acquired image and reference image (to correct for stage inaccuracy)
compare/difference acquired image with reference image
report differences/defects
move to next adjacent position
wait for stage to settle
UNTIL area to be imaged is complete
report or display defects (for example, in KLA wafer-map format)

2. Step-and-image with large-FOV objective lens (Assumes reference images have already been acquired using the sane or similar procedure.)

Load wafer, pump down, align wafer (optical and or e-beam), align die (also optical and or e-beam)
Set up imaging parameters, energy, current, focus, astigmatism, area to be imaged, wafer, extraction and filter biases, image processing algorithm (typically all stored in a wafer recipe database)
REPEAT (acquire all images for the areas) requested by the user)
REPEAT (acquire all images for a single stage position with large-FOV objective lens)
deflect beam to sub-FOV
set/adjust imaging parameters (focus, stig, XY offset—from pre determined lookup table . . .)
(optionally) pre-charge with flood gun (using the multiplexing 1
acquire & store sub-FOV image (for example, 1000 pixels×1000 pixels)
IF reference image available (ideally in parallel with setup and acquisition of next image)
align acquired image 8t reference image (see Alignment Note below)
compare/difference acquired image with reference image
report differences/defects
UNTIL all sub-FOV images for this stage position acquired

Patent provided by Sughrue Mion, PLLC - http://www.sughrue.com

move to next adjacent XY stage position OR next die IF current die complete
wait for stage to settle
UNTIL area to be imaged is complete
report or display defects (for example, in KLA results file defect wafer map format)

Step and Image Alignment Note: 2–3 pixels using convolution or other algorithms—to correct for stage inaccuracy. Position or alignment repeatability of the large-FOV lens is likely to be high thus this alignment step may only be necessary on a few of the several hundred sub-FOV images acquired for each mechanical stage position. The alignment offset from neighboring images will in many cases be sufficient for alignment. A typical or likely approach might be to align only the first and last image from a set of sub-FOV images and to interpolate between these alignment offsets for all other images in the sub-FOV set.

In one embodiment of the invention, the whole of the larger FOV (e.g., greater than 100 mm across with a substantially uniform resolution over the FOV) can be acquired as a single image by applying dynamic astigmatism and focus corrections as is common in e-beam lithography systems. While this is more complex to implement than the sub-FOV imaging embodiment, it nevertheless can overcome the stage overhead problem.

Although experience to date suggests that voltage-contrast-based defect detection is a valuable mode of operation, some defects on some layers of a multi-layer wafer can only be detected with conventional SEM-style imaging; these include pattern defects, such as extra or missing pattern, that do not cause an open or short or do not change the voltage-contrast state of the associated features. There is little difference in the operation of the system when looking for these defects except that the wafer bias and extraction control parameters are no longer adjusted to maximize the voltage-contrast signal. Instead, the biases are set to zero or are set to maximize topographic contrast. Moreover, pattern defects can be significantly smaller than the minimum critical dimension of circuit feature size and higher magnification (more pixels per micron) may be required for reliable operation. The actual settings will vary depending on the material and layer inspected.

In a simple implementation consistent with the invention it is not necessary to use a flood beam. Pre-charging the sample by flooding the wafer has the advantages of requiring less beam time to obtain an image having good voltage contrast, and more uniform contrast due to a more uniform charge distribution within the imaged area as well as the surrounding area. Non-uniform charging in the area surrounding the imaged area can result in contrast variations across the field of view and increased false and nuisance defects. In a system equipped with a flood gun, a simple mode of operation is to pre-charge each sub-FOV with the flood beam prior to acquiring an image of that sub-FOV with the focused beam. This saves time due to faster charging than is possible with the focused beam but has the disadvantage of incurring a flood-beam-multiplexing overhead of tens to hundreds of microseconds per sub-FOV. If leakage currents on the wafer being inspected are low relative to the capacitance of the features to be imaged, flooding of multiple sub-FOVs can reduce the overhead per sub-FOV. Typical wafers inspected have had a discharge time constant from many tens of milliseconds to a few seconds. The typical frame rate is 10 ms to 100 ms per frame, so pre-charge flooding of a few sub-FOVs is a practical means to reducing multiplexing overhead. For large features such as bond pads and power planes that are typically on the uppermost metal layers, pre-charge flood of the whole FOV is possible. The flood gun implementation described can have a flood spot size on the order of ~100 μm across and so the flood beam must be raster scanned to cover the entire FOV of the large-FOV objective lens, which may be ~1 mm across.

A limiting factor in the speed of any e-beam-based detection system is the amount of beam current delivered to the sample, assuming that the video signal is processed perfectly, that image-processing algorithms are fully optimized, and that the best sampling plan is being applied. We have thus far described single-column implementation consistent with the invention. For large wafers (e.g., 200 mm and 300 mm diameter wafers), two or four or more columns can be mounted on the system together and used in parallel to increase the overall area coverage rate of the system. Each column in used in the step-and-image mode to image sub-FOVs. Each column may have its own set of support electronics and image-processing hardware. While more costly than a single-column system, a multiple-column system is expected to be less costly than multiple single-column systems because the mechanical stage, vacuum chamber, robot, user-interface computer, etc., are shared.

FIG. **9** shows a schematic, plan view of a defect-detection system consistent with the invention having two columns ganged together for simultaneously imaging multiple regions of a wafer. Columns **900** and **905** are shown relative to a wafer **910** mounted on a wafer chuck **915** on an x-stage **920** and a y-stage **925**.

FIG. **10** shows a schematic, plan view of a defect-detection system consistent with the invention having four columns ganged together for simultaneously imaging multiple regions of a wafer. Columns **1000**, **1005**, **1010** and **1015** are shown relative to a wafer **1020** mounted on a wafer chuck **1025** on an x-stage **1030** and a y-stage **1035**.

FIG. **11** shows a schematic, plan view of a defect-detection system consistent with the invention having nine columns ganged together for simultaneously imaging multiple regions of a wafer. Columns **1100**, **1105**, **1110**, **1115**, **1120**, **1125**, **1130**, **1135** and **1140** are shown relative to a wafer **1145** mounted on a wafer chuck **1150** on an x-stage **1155** and a y-stage **1160**.

FIG. **12** shows a schematic view of a defect-detection system **1200** consistent with the invention having two columns ganged together for simultaneously imaging multiple regions of a wafer. A first column **1205** has a gun ion pump **1210**, flood gun **1215**, detector **1220** and large-FOV objective lens **1225**. Provided for column **1205** are control electronics **1230** and image-capture and processing electronics **1235** in communication via bus **1240** with a control computer **1245** having a display **1250**. A second column **1255** likewise has a gun ion pump, flood gun, detector and large-FOV objective lens. Provided for column **1255** are control electronics **1260** and image-capture and processing electronics **1265** in communication via bus **1240** with control computer **1245**. Columns **1205** and **1255** can be operated simultaneously to image regions of a wafer **1270** carried by a wafer chuck **1275** on an X-Y stage **1280** in a vacuum chamber **1285**. The system is also equipped with turbo pump **1288** for evacuating chamber **1285**, active vibration isolation platform **1290**, wafer-handling equipment **1292** (including a vacuum load lock and wafer-handling robots), and wafer cassette **1295**.

The description given above is for an e-beam imaging system, though a system consistent with the invention can alternately employ an ion beam such as a hydrogen-ion beam or other non-Gallium-ion beam. The term "charged-

Patent provided by Sughrue Mion, PLLC - http://www.sughrue.com

particle beam" is intended to include an e-beam as well as an ion beam other than a Gallium-ion beam.

Those of skill in the art will recognize that these and other modifications can be made within the spirit and scope of the invention as defined in the claims.

What is claimed is:

1. A method of detecting defects in a patterned substrate, comprising:

operating a charged-particle-beam optical column so as to acquire a plurality of images of a region of the patterned substrate having a width of greater than approximately 100 μm without moving the charged-particle-beam optical column relative to the patterned substrate; and

comparing the acquired images to a reference to identify defects in the patterned substrate.

2. The method of claim **1**, wherein the charged-particle-beam column includes an electron-beam source.

3. The method of claim **2**, where in the electron-beam source includes a thermal-field-emission cathode.

4. The method of claim **2**, wherein the electron-beam source includes a zirconium-tungsten cathode.

5. The method of claim **1**, further comprising monitoring a position of the patterned substrate with a laser interferometer.

6. The method of claim **1**, wherein operating the charged-particle-beam optical column to acquire images comprises acquiring voltage-contrast images.

7. The method of claim **1**, further comprising applying charged particles to pre-charge the patterned substrate prior to operating the charged-particle-beam optical column to acquire images.

8. The method of claim **1**, wherein operating the charged-particle-beam optical column to acquire images comprises acquiring topographic images, and wherein comparing comprises comparing the acquired images to a reference to identify topographic defects in the patterned substrate.

9. The method of claim **1**, wherein the reference comprises an image of a portion of the patterned substrate.

10. The method of claim **1**, wherein the reference comprises a stored reference image.

11. The method of claim **1**, wherein the reference comprises an image generated from a computer-aided-design (CAD) database.

12. The method of claim **1**, wherein the comparing comprises comparing features of the acquired images with features of a reference to identify defects in the patterned substrate.

13. The method of claim **1**, wherein the acquired images are comprised of pixels and the reference is a reference image comprised of pixels, and wherein comparing the acquired images comprises comparing the acquired images pixel-by-pixel with the reference image.

14. The method of claim **1**, further comprising applying a flood beam to the patterned substrate prior to operating the charged-particle-beam optical column to acquire images.

15. The method of claim **14**, wherein applying the flood beam to the patterned substrate comprises applying the flood beam to a sub-area of the FOV.

16. The method of claim **1**, wherein the charged-particle-beam optical column comprises a variable-axis immersion lens (VAIL).

17. The method of claim **1**, wherein the charged-particle-beam optical column includes an in-lens charged-particle detector for collecting and detecting secondary particles substantially uniformly across the FOV.

18. The method of claim **1**, further comprising:

positioning a second charge-particle-beam optical column relative to the patterned substrate, the second charged-particle optical column having a field of view (FOV) with a substantially uniform resolution over the FOV;

operating the second charged-particle-beam optical column to acquire second images over multiple subareas of a region of the patterned substrate lying within the FOV by scanning the second charged-particle beam over the patterned substrate; and

comparing the acquired second images to a reference to identify defects in the patterned substrate.

* * * * *

Patent provided by Sughrue Mion, PLLC - http://www.sughrue.com